The Japan Society of Mechanical Engineers

Lattice Strain and Domain Switching Induced in Tetragonal PZT by Poling and Mechanical Loading*

Keisuke TANAKA**, Yoshiaki AKINIWA**,
Yoshihisa SAKAIDA*** and Hirohisa KIMACHI**

The X-ray diffraction method was applied to measure the change of the lattice strain and domain switching in tetragonal lead zirconate titanate (PZT) due to poling and external mechanical loading. The lattice strain was determined from the linear relation between the diffraction angle and $\sin^2\psi$ (ψ is the angle between the normals of the diffraction plane and the specimen surface). The lattice strain measured by X-rays is less than 50% of the macrostrain determined from the dimensional change due to poling. The applied strain induced the increase of the lattice strain, and the amount of increase was about 50% of the applied strain. The amount of domain switching was evaluated by the change of the intensity ratio of 002 to 200 diffraction. The intensity ratio was decreased with the applied strain. The broadening of X-ray diffraction profiles obtained from the diffraction plane perpendicular to the poling direction was the maximum, indicating the largest microstrain in the poling direction.

Key Words: Experimental Stress Analysis, Residual Stress, Ceramics, Bending, X-Ray Strain Measurement, Lead Zirconate Titanate, Polarization, Domain Switching, Lattice Strain, Microstrain

1. Introduction

Lead titanate zirconate (PZT) is the most commonly used piezoelectric ceramics for sensors and actuators. Its strength properties as well as piezoelectric properties should be guaranteed especially when used as actuators at high power. PZT has a perovskite structure of $Pb(Zr, Ti)O_3$ and the crystalline structure is either tetragonal or rhombohedral structures at about equal fraction of zirconium and titanium[1]. The poling treatment introduces the lattice strain and the switching of domain structure in PZT[2),(3)]. In the present paper, the X-ray diffraction method is used to investigate the lattice strain and domain switching induced in tetragonal PZT by poling and external mechanical stressing.

* Received 7th January, 2000
** Department of Mechanical Engineering, Nagoya University, Furo-cho, Chikusa-ku, Nagoya 464-8603, Japan. E-mail: k_tanaka@mech. nagoya-u. ac. jp
*** Japan Fine Ceramics Center, Atsuta-ku, Nagoya 456-8587, Japan

2. Experimental Procedure

2.1 Material and specimens

The experimental material of PZT was pressureless sintered at 1 503 K to have a tetragonal structure. The atomic fractions of Zr and Ti are 53 and 47 at %, respectively. The lattice constants of the tetragonal structure determined by X-rays are $a=0.40410$ nm and $c=0.41087$ nm. The spontaneous polarization direction is the c axis. Two types of specimens were used: the one had a rectangular cross section of 4.1 mm and 10 mm with a length of 65 mm, the other a cross section of 3.5 mm and 10 mm with a length of 40 mm. The former specimens were used for poling in T and S directions, and the latter in L direction (see Fig. 1). They are shaped by grinding with #800 diamond wheel, and the surface of 10 mm times 65 mm (or 40 mm) was finished by lapping for X-ray measurements. After machined, all specimens were annealed at 673 K for 10 min in air.

Some specimens were poled at 373 K in silicon oil. Figure 1 indicates three directions, L, T and S, in the rectangular specimen, and the poling was conducted in L, T and S directions. The voltage of the direct

NII-Electronic Library Service

The Japan Society of Mechanical Engineers

Table 1 X-ray conditions for tetragonal PZT

Equipment	MXP-18		XD-D1
Method	Parallel beam method		Focusing beam method
Characteristic X-ray	CrK_α	CrK_α	CuK_α
Filter	Vanadium	Vanadium	Monochromator
Diffraction line	222	002 200	222
Diffraction angle (deg)	154.8	67.88 69.04	81.89
Tube voltage (kV)	30	30	40
Tube current (mA)	200	200	30
Scanning speed (deg/min)	1.00	0.50	0.50
Sampling interval (deg)	0.05	0.05	0.02

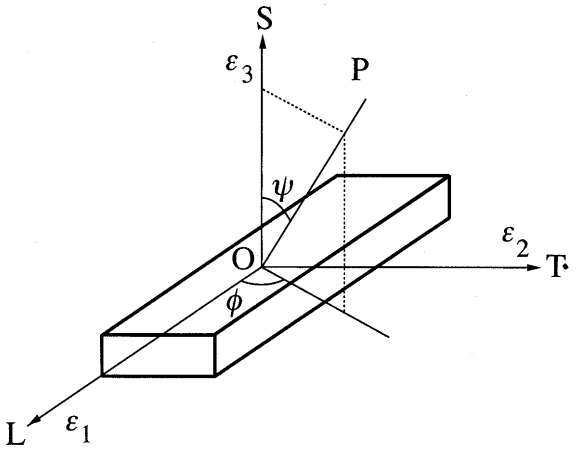

Fig. 1 Poling directions L, T and S in specimen

current used for poling was 48 kV for L direction, 19 kV for T direction and 7.8 kV for S direction. The poling period was 10 min. In the following, the specimens poled in L, T, and S direction are called PL, PT, and PS specimens, respectively. Those not poled are designated by NP specimens.

2.2 X-Ray measurement of lattice strain

The X-ray equipment used was a high power X-ray generator (MAC Science MXP-18) with a rotating Cr anode operated at a tube voltage of 30 kV and a tube current of 200 mA. The diffraction conditions for strain measurements are summarized in Table 1. The 222 diffraction was used. The peak position was determined at the diffraction angle at the middle of the full width at 80% of the maximum of the diffraction profile after eliminating the diffraction due to $K_{\alpha 2}$ radiation. The parallel beam optics was adopted in a Ω goniometer (iso-inclination) arrangement.

The lattice strain ε is measured by the change of the diffraction angle 2θ as follows[4]:

$$\varepsilon=-\cot\theta_0(\theta-\theta_0) \qquad (1)$$

where $2\theta_0$ is the diffraction angle from the strain-free material.

The principal strains corresponding to L, T, S directions are denoted by ε_1, ε_2 and ε_3 as shown in Fig. 1. The normal strain ε_ψ in OP direction is expressed by

$$\varepsilon_\psi=(\varepsilon_1\cos^2\phi+\varepsilon_2\sin^2\phi-\varepsilon_3)\sin^2\psi+\varepsilon_3 \qquad (2)$$

For the case of $\phi=0°$, we have

$$\varepsilon_\psi=(\varepsilon_1-\varepsilon_3)\sin^2\psi+\varepsilon_3 \qquad (3)$$

The substitution of Eq.(1) into Eq.(3) gives

$$2\theta=-2\tan\theta_0(\varepsilon_1-\varepsilon_3)\sin^2\psi-2\tan\theta_0\varepsilon_3+2\theta_0 \qquad (4)$$

A similar equation can be obtained for the case of $\phi=90°$ as follows:

$$2\theta=-2\tan\theta_0(\varepsilon_2-\varepsilon_3)\sin^2\psi-2\tan\theta_0\varepsilon_3+2\theta_0 \qquad (5)$$

From the slope of the linear relation between 2θ and $\sin^2\psi$, the strain difference of $\varepsilon_1-\varepsilon_3$ or $\varepsilon_2-\varepsilon_3$ can be determined. Once the diffraction angle of the strain-free material, $2\theta_0$, is obtained, each value of ε_1, ε_2 and ε_3 can be separated.

2.3 X-Ray measurement of lattice strain under external stress

The four-point bending stress was applied to L direction, and the strain value was monitored from the strain gage glued on the tension side of the specimen. The X-ray measurement was conducted after keeping 20 min at prescribed strains, and the relation between the load and the strain was recorded during the test.

2.4 Measurements of intensity and line broadening

The spontaneous polarization axis of tetragonal crystals is 001 direction (the c axis). The amount of domain switching can be evaluated from the intensity ratio of 002 to 200 diffraction[5],[6]. Since the diffraction profiles of 002 and 200 are overlapped, the wave separation was conducted after subtracting the diffraction by $K_{\alpha 2}$ radiation from the measured profile.

The line broadening of diffraction profiles was measured for 222 diffraction. After subtracting the diffraction by $K_{\alpha 2}$ from the original profile, the full width at 80% of the maximum was measured. To perform a more accurate measurement of the line broadening, the focusing beam was used. A monochromator was attached to the detection side of the X-ray equipment (Shimadzu XD-D1). The full-width at the half maximum of 222 diffraction by CuK_α radiation was measured after eliminating the

NII-Electronic Library Service

The Japan Society of Mechanical Engineers

Table 2 Strains in poled tetragonal PZT

Material	PL			PT			PS		
	ε_1	ε_2	ε_3	ε_1	ε_2	ε_3	ε_1	ε_2	ε_3
Strain measured by dimensional change, ε_T ($\times 10^{-6}$)	2760	−1000	−1000	−1000	2030	−1000	−1400	−1400	3660
Strain measured by X-ray for (222), ε_X ($\times 10^{-6}$)	230	−300	−170	−500	560	−290	−660	−710	1190
Strain due to domain switching, ε_D ($\times 10^{-6}$)	2530	−700	−830	−500	1470	−710	−740	−690	2470

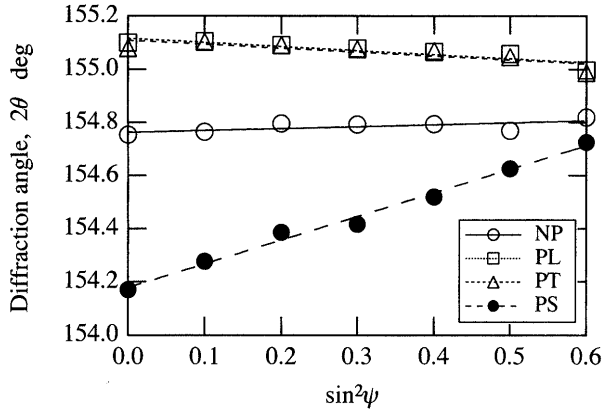

(a) L direction

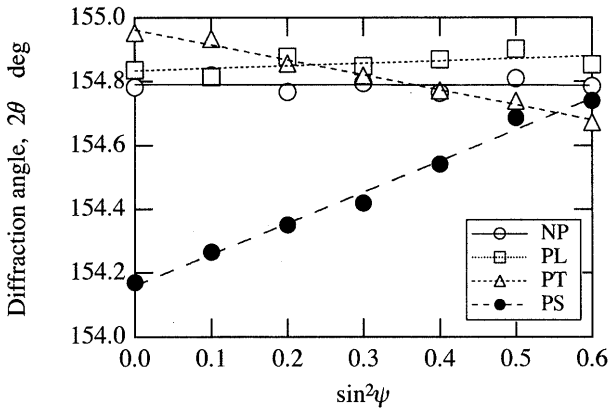

(b) T direction

Fig. 2 Relation between diffraction angle and $\sin^2\psi$ for 222 diffraction of tetragonal PZT

diffraction by $K_{\alpha 2}$ radiation from the measured profile.

3. Experimental Results and Discussion

3.1 Lattice strain in poled PZT

The relation between the diffraction angle 2θ and $\sin^2\psi$ is shown in Fig. 2 for NP, PL, PT and PS specimens, where ψ is the angle inclined to L direction ($\phi=0°$ in Fig. 1) in the case of (a) and to T direction ($\phi=90°$ in Fig. 1) in the case of (b). The relation can be approximated by a linear relation for each specimen. It should be noted that the poling treatment induces the macroscopic lattice strain, even if there is no macrostress acting. The relation for NP specimens is nearly flat, suggesting no macrostrain. The diffraction angle for strain-free materials is taken as the mean of the diffraction angles at the intercept between the ordinate and the linear regression line of the $2\theta-\sin^2\psi$ relation for NP specimens for L and T directions. The three components of strains can be determined using Eqs. (4) and (5).

Table 2 summarizes the measured X-ray lattice strain, ε_X. The lattice strain is tensile in the direction of poling, and compressive in the perpendicular direction. The poling treatment introduced the dimensional change of the specimen. This strain denoted by ε_T is also shown in the table. The dimensional change of the specimen is the sum of the lattice strain, ε_X, and the strain, ε_D, caused by domain switching[7]. The strain due to domain switching is determined by

$$\varepsilon_D=\varepsilon_T-\varepsilon_X \quad (6)$$

The determined value of ε_D is presented in Table 2. The major part of ε_T comes from domain switching. The X-ray lattice strain is caused by poling and also by the applied stress as described later. Therefore, the X-ray strain is the sum of two strain components: one due to poling and the other due to elastic deformation as

$$\varepsilon_X=(\varepsilon_X)_P+(\varepsilon_X)_E \quad (7)$$

Since the lattice strain can be introduced by poling as well as by external stress, it may be difficult to discriminate $(\varepsilon_X)_E$ from $(\varepsilon_X)_P$ to determine the residual stress in piezoelectric ceramics.

3.2 Effect of loading on lattice strain

The relation between the applied stress and the strain is shown in Fig. 3, the applied stress taken as the ordinate is the nominal stress calculated from the load by using the elementary equation of the strength of materials under the assumption of linear elasticity. The relation is linear up to about 200×10^{-6} strain, and then becomes nonlinear. The relation during unloading follows a different relation, forming a hysteresis loop. When the strain is held at a constant value, the stress decreases during the loading process, while increases during the unloading process. This is caused by the time-dependent delayed switching of domains. The amount of stress change during the strain hold is smallest for NP specimens and largest for PS

NII-Electronic Library Service

The Japan Society of Mechanical Engineers

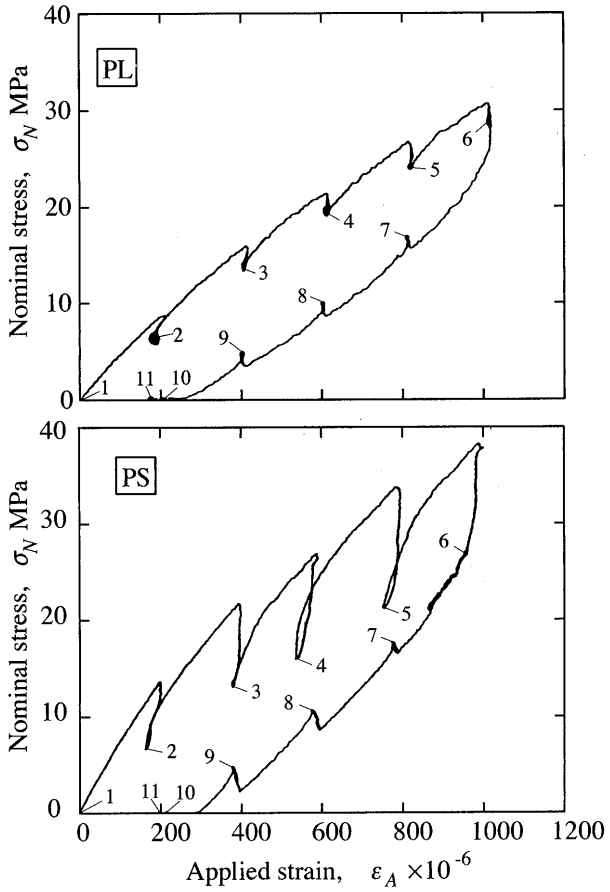

Fig. 3 Stress vs. strain relation during X-ray measurement

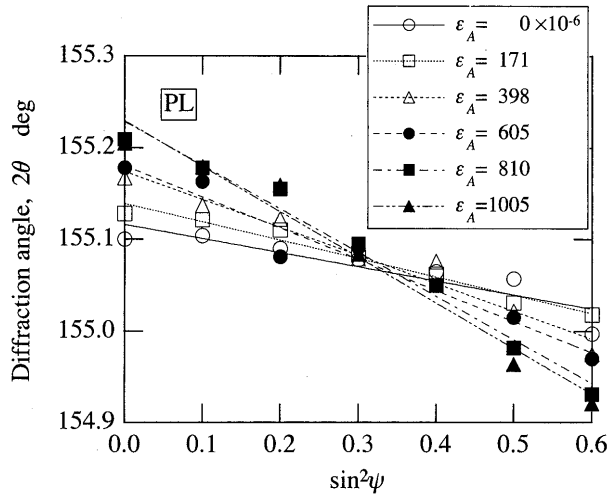

Fig. 4 Relation between diffraction angle and $\sin^2\psi$ for PL specimen

specimens.

Figure 4 shows the effect of the applied strain on the relation between 2θ and $\sin^2\psi$ for PL specimen. The slope of the linear regression line decreases with increasing strain. After unloading, the slope increases, but does not come back to the initial value. Some amount of residuals of the domain switching and lattice strain were left in PZT. In Fig. 5, the changes of the slope and the intercept are plotted against the applied strain, where the open marks indicate the data for loading and the solid marks for unloading. Both values change linearly with the applied strain.

Table 3 Change of lattice strain due to applied strain

Material	NP	PL	PT	PS
$\partial(\varepsilon_1-\varepsilon_3)/\partial\varepsilon_A$	0.875	0.730	0.956	0.961
$\partial\varepsilon_3/\partial\varepsilon_A$	−0.340	−0.255	−0.281	−0.468
$\partial\varepsilon_1/\partial\varepsilon_A$	0.534	0.475	0.675	0.492
$-\partial\varepsilon_3/\partial\varepsilon_1$	0.636	0.537	0.416	0.952

From Eq. (4), the change of lattice strains with the applied strain, ε_A, is determined as follows:

$$\frac{\partial(\varepsilon_1-\varepsilon_3)}{\partial\varepsilon_A}=-\frac{\cot\theta_0}{2}\left(\frac{\partial M}{\partial\varepsilon_A}\right) \quad (8)$$

$$\frac{\partial\varepsilon_3}{\partial\varepsilon_A}=-\frac{\cot\theta_0}{2}\left(\frac{\partial(2\theta_{\psi=0})}{\partial\varepsilon_A}\right) \quad (9)$$

where M is the slope in the 2θ vs. $\sin^2\psi$ relation and $2\theta_{\psi=0}$ is the diffraction angle at $\psi=0°$. From the linear regression line for loading data shown in Fig. 5, the change of strains with the applied strain was determined by using Eqs. (8) and (9).

The results are summarized in Table 3. The value of $\partial\varepsilon_1/\partial\varepsilon_A$ is nearly 0.5. The value of $-\partial\varepsilon_3/\partial\varepsilon_1$, corresponding to Poisson's ratio, is about 1 for PS specimens, and about 0.5 for the other specimens.

3.3 Intensity ratio of 002 to 200 diffraction

The intensity ratio of 002 diffraction to 200 diffraction was measured for the normal incidence ($\psi=0°$). Figure 6 shows the X-ray profiles for PL and PS specimens without loading, where the background and the diffraction by $K_{\alpha 2}$ are subtracted from the original profiles. The solid line is the original profile, and the dash-dotted line and the dashed line are the decomposed profiles of 002 and 200 diffractions. The dotted line is the profile composed of 002 and 200 (decomposed) diffractions. The 002 diffraction is at the lower angle and the 200 diffraction at the higher angle. The 002 diffraction is stronger for PS specimens, while weaker for PL specimens. This is because the poling treatment aligns the spontaneous polarization direction (the c axis) of domains along the poling direction.

Figure 7 indicates the change of the intensity ratio due to the applied strain for NP, PT, PL and PS specimens. With increasing strain, the intensity ratio decreases, because the c axis turns to the loading direction. By unloading, the intensity ratio recovers. The amount of change is large for PS specimens, while small for PL and PT specimens.

NII-Electronic Library Service

The Japan Society of Mechanical Engineers

3.4 X-Ray line broadening

The line broadening of diffraction profiles corresponds to the microstrain or the inhomogeneous part of the lattice strain. The full width, B_{80}, at 80% of the maximum of 222 diffraction by CrK_α as measured for the case of $\psi=0°$. Table 4 summarizes the data of B_{80}. The resolution of line broadening is higher for the focusing method than for the parallel beam method. The full width, B_{50}, at the half maximum measured for 222 diffraction by CuK_α radiation with the focusing method is also presented in Table 4. The value for the focusing beam method is smaller than that for the parallel beam method. The width is the largest for PS specimens. The width for PL and PT specimens is slightly smaller than that for NP specimens.

A large microstrain perpendicular to the poling direction is explained as follows. Before poling, the polarization of domains is oriented randomly. The poling process induces the domain switching and extends the switched domain. The switched domain is

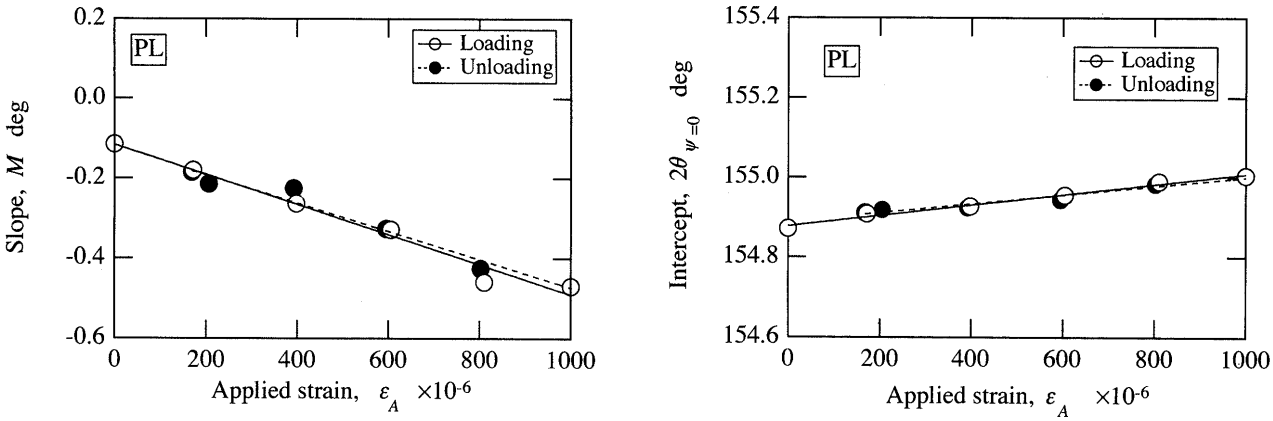

(a) Slope vs. strain (b) Intercept vs. strain

Fig. 5 Changes of slope and intercept with applied strain of PL specimen

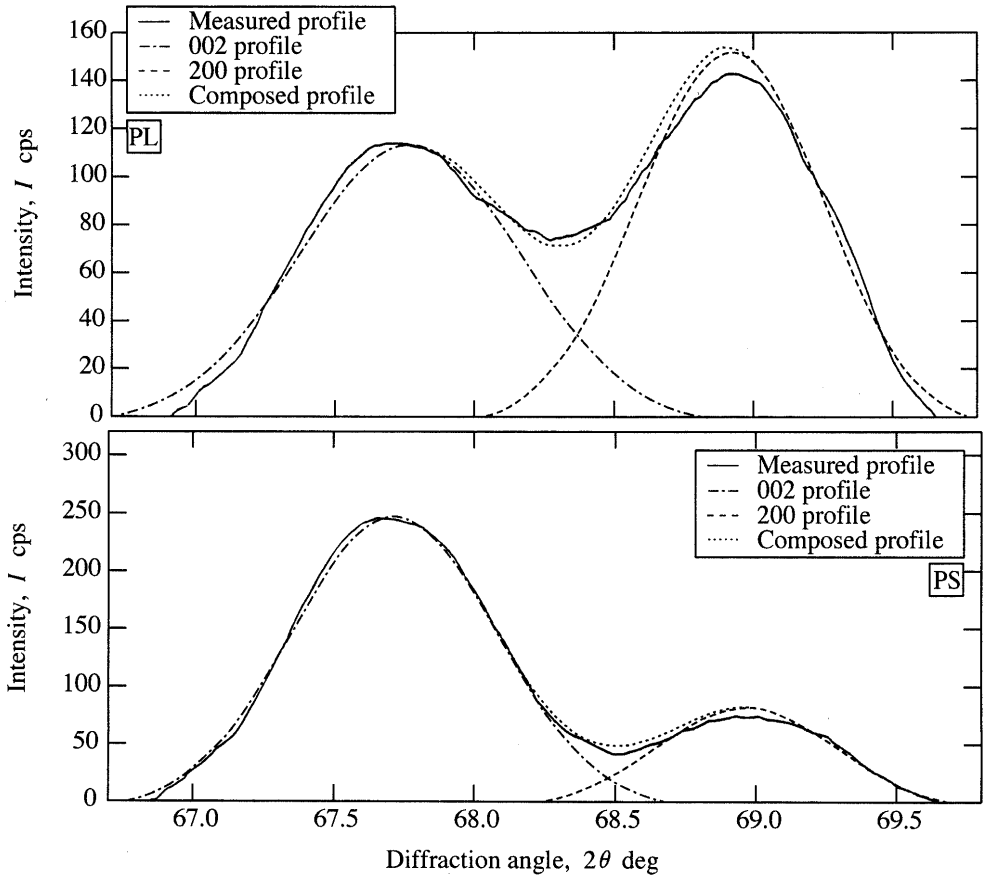

Fig. 6 X-ray diffraction profile of tetragonal PZT

NII-Electronic Library Service

The Japan Society of Mechanical Engineers

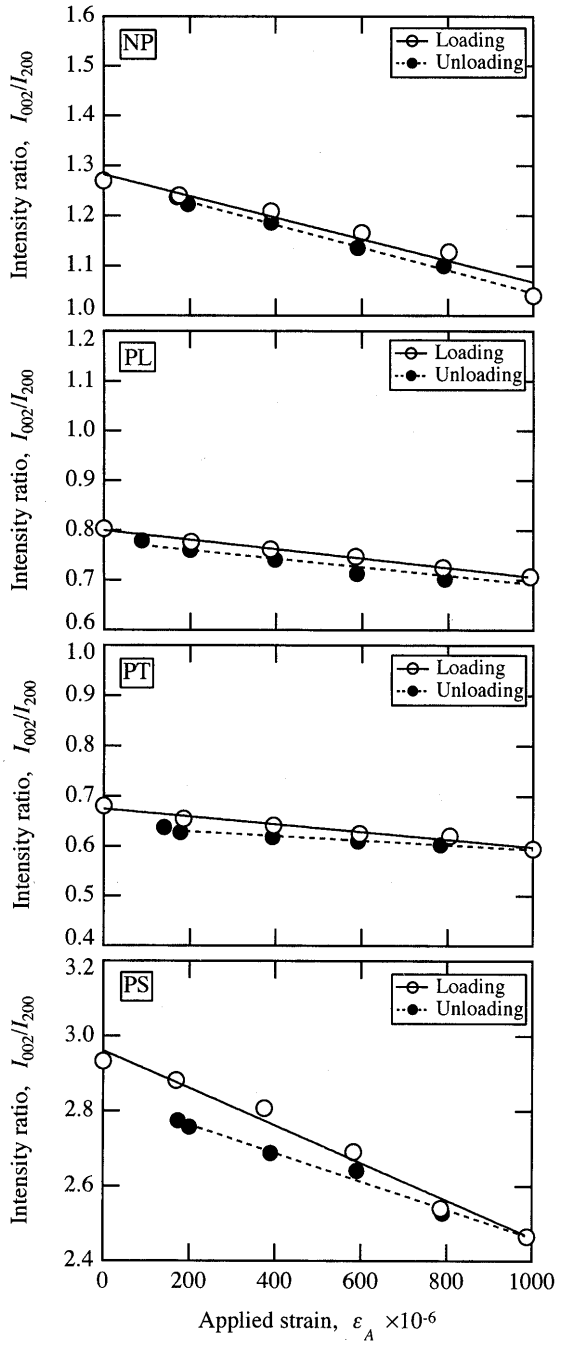

Fig. 7 Change of intensity ratio with applied strain for tetragonal PZT

subjected to compressive strain because of the constraint by surrounding domains. The surrounding domains are now under tension in order to balance the internal stress. The variation of the lattice strain will be maximum in the poling direction, thus the line broadening becomes the largest.

Figure 8 shows the change of B_{80} with the applied strain. The width tends to decrease with the applied strain, but the amount of change is very small. The amount of domain switching induced by loading is not so large as that by poling.

Table 4 X-ray line broadening of 222 diffraction of tetragonal PZT

Specimen	NP	PL	PT	PS
Parallel beam method B_{80}(deg)	1.324	1.303	1.241	1.480
Focusing beam method B_{50}(deg)	0.403	0.392	0.399	0.442

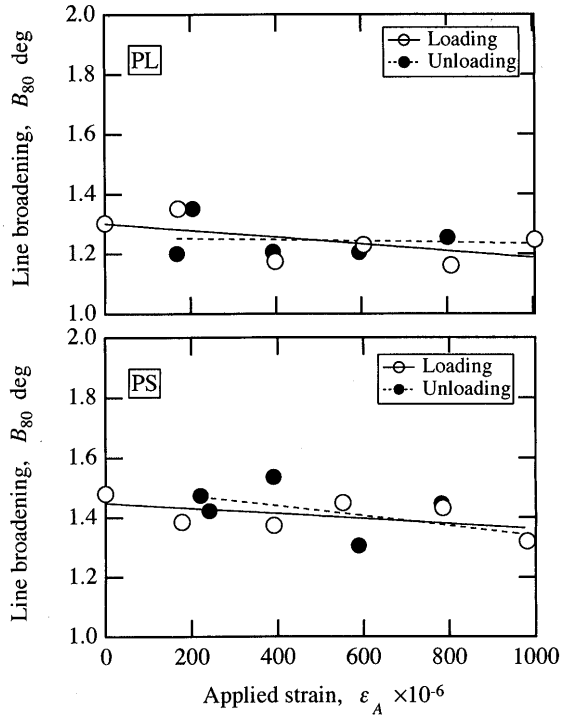

Fig. 8 Variation of line broadening with applied strain for tetragonal PZT

4. Conclusions

(1) The lattice strain measured by X-rays is extension in the poling direction and contraction in the perpendicular direction. The magnitude of the lattice strain measured by X-rays is much smaller than the strain determined from dimensional change.

(2) External loading induces domain switching and lattice strains in PZT. The change of the lattice strain in the loading direction is about 50% of the applied strain. The ratio of the short-transverse strain to the longitudinal strain is about minus one for PS specimens and about −0.5 for the other specimens.

(3) The intensity ratio of 002 diffraction to 200 diffraction corresponds to the amount of domain switching. The intensity ratio decreases with increasing strain, and recovered after unloading.

(4) The broadening of X-ray diffraction profiles obtained from the diffraction plane perpendicular to the poling direction was the maximum, indicating the largest microstrain in the poling direction.

NII-Electronic Library Service

The Japan Society of Mechanical Engineers

References

(1) Kakegawa, K., Mohri, J., Takahashi, T., Yamamura, H. and Shirasaki, S., A Compositional Fluctuation and Properties of $Pb(Zr, Ti)O_3$, Solid State Comm., Vol. 24 (1977), pp. 769-772.

(2) Uchida, N. and Ikeda, T., Electrostriction in Perovskite-Type Ferroelectric Ceramics, Jpn. J. Appl. Phys., Vol. 6 (1967), pp. 1079-1088.

(3) Tanaka, K., Sakaida, Y., Nomura, H. and Akiniwa, Y., X-Ray Study of Lattice Strain in Piezoelectric Ceramics (PZT), Proc. 5th Inter. Conf. Residual Stresses, edited by Ericsson, T., Oden, M. and Andersson, A., Vol. 1 (1997), pp. 232-237.

(4) Noyan, I.C. and Cohen, J.B., Residual Stress, (1987), p. 117, Springer.

(5) Mehta, K. and Virkar, A.V., Fracture Mechanisms in Ferroelectric-Ferroelastic Lead Zirconate Titanate (Zr : Ti=0.54 : 0.46) Ceramics, J. Am. Ceram. Soci., Vol. 73 (1990), pp. 567-574.

(6) Saito, Y., Hysteresis Curve of X-Ray Diffraction Peak Intensity in Lead Zirconate Titanate Ceramics, Jpn. J. Appl. Phy., Vol. 36 (1997), pp. 5963-5969.

(7) Cao, H. and Evans, A.G., Nonlinear Deformation of Ferroelectric Ceramics, J. Am. Ceram. Soci., Vol. 76 (1993), pp. 890-896.

NII-Electronic Library Service